JOURNAL OF VIROLOGY, Oct. 2000, p. 9655–9667 Vol. 74, No. 20
0022-538X/00/$04.00+0
Copyright © 2000, American Society for Microbiology. All Rights Reserved.

Internalization of Adenovirus by Alveolar Macrophages Initiates Early Proinflammatory Signaling during Acute Respiratory Tract Infection

ZSUZSANNA ZSENGELLÉR,[1]† KAZUHISA OTAKE,[1]‡ SHAIKH-ABU HOSSAIN,[1] PIERRE-YVES BERCLAZ,[2] AND BRUCE C. TRAPNELL[1]*

Division of Pulmonary Biology[1] and Division of Pulmonary Medicine,[2] Children's Hospital Medical Center, Cincinnati, Ohio 45229

Received 30 March 2000/Accepted 13 July 2000

Adenovirus is a common respiratory pathogen which causes a broad range of distinct clinical syndromes and has recently received attention for its potential for in vivo gene delivery. Although adenovirus respiratory tract infection (ARTI) results in dose-dependent, local inflammation, the pathogenesis of this remains unclear. We hypothesized that alveolar macrophages (AMϕ) rapidly internalize adenovirus following in vivo pulmonary administration and then initiate inflammatory signaling within the lung. To evaluate the role of AMϕ in the induction of lung inflammation during ARTI in vivo, we directly assessed adenovirus uptake by murine AMϕ and correlated uptake with the initiation of proinflammatory gene expression. Stimulation of cytokine (tumor necrosis factor alpha [TNF-α], interleukin-6 [IL-6], macrophage inflammatory protein-2 [MIP-2], and MIP-1α) expression in the lung was evaluated at the level of mRNA (by reverse transcription-PCR [RT-PCR]) and protein (by enzyme-linked immunosorbent assay) and by identification of cells expressing TNF-α and IL-6 mRNA in lung tissues (by in situ hybridization) and isolated lung lavage cells (by RT-PCR). Adenovirus, labeled with the fluorescent dye (Cy3), was rapidly and widely distributed on epithelial surfaces of airways and alveoli and was very rapidly (~1 min) localized within AMϕ. At 30 min after infection AMϕ but not airway epithelial or vascular endothelial cells expressed mRNA for TNF-α and IL-6, thus identifying AMϕ as the cell source of initial cytokine signaling. IL-6, TNF-α, MIP-2, and MIP-1α levels progressively increased in bronchoalveolar lavage fluid after pulmonary adenovirus infection, and all were significantly elevated at 6 h ($P < 0.05$). To begin to define the molecular mechanism(s) by which adenovirus initiates the inflammatory signaling in macrophages, TNF-α expression from adenovirus-infected RAW264.7 macrophages was evaluated in vitro. TNF-α expression was readily detected in adenovirus-infected RAW cell supernatant with kinetics similar to AMϕ during in vivo infection. Blockage of virus uptake at specific cellular sites, including internalization (by wortmannin), endosome acidification and/or lysis (by chloroquine) or by Ca^{2+} chelation (by BAPTA) completely blocked TNF-α expression. In conclusion, results showed that during ARTI, (i) AMϕ rapidly internalized adenovirus, (ii) expression of inflammatory mediators was initiated within AMϕ and not airway epithelial or other cells, and (iii) the initiation of inflammatory signaling was linked to virion uptake by macrophages occurring at a point after vesicle acidification. These results have implications for our understanding of the role of the AMϕ in the initiation of inflammation following adenovirus infection and adenovirus-mediated gene transfer to the lung.

Adenovirus, a nonenveloped DNA virus with at least 45 serotypes, is an important respiratory pathogen affecting individuals of all ages and accounting for 7 to 10% of all respiratory illnesses in infants and children, with an incidence of between 5 to 10 million infections annually in the United States alone (13, 21). Adenovirus respiratory tract infection (ARTI) occurs sporadically, epidemically, and nosocomially, presents in a wide spectrum of distinct clinical syndromes ranging from self-limited acute pharyngitis to fatal pneumonia, and has been identified as an etiological factor associated with exacerbations in individuals with chronic obstructive lung diseases (13). Despite the frequency and broad range of clinical presentations, the pathogenesis of inflammation in ARTI is poorly understood. Early information regarding host responses to adenovirus was derived from efforts to develop human adenovirus vaccines (42) or to understand the pathology of fatal adenoviral pneumonia (4). Recently, ARTI has been studied in a variety of animal models, including mice (14, 37, 58), Cotton rats (*Sigmodon hispidus*) (15, 39, 59, 60), and primates (8, 44, 55, 61) as part of preclinical toxicology studies for human gene therapy clinical trials for cystic fibrosis (reviewed in references 7 and 48). Studies in humans showed that administration of replication-deficient adenovirus vectors to the respiratory tract can cause dose-dependent local inflammation (12, 26, 33).

Inflammatory responses to ARTI have been best studied in rodent models. In the Cotton rat, a permissive host for replication of human adenovirus, pulmonary histopathology consists of early and late phases similar to that seen in human ARTI (15, 39). The early phase consists primarily of accumulation of neutrophils, macrophages, and monocytes and develops within the first 24 h (60). The late phase, consisting mainly of lymphocytes, is apparent by day 5 (39, 60). In mice, a nonpermissive host for human adenovirus, adenovirus early gene

* Corresponding author. Mailing address: Children's Hospital Medical Center, Division of Pulmonary Biology, 3333 Burnet Ave., Cincinnati, OH 45229. Phone: (513) 636-6361. Fax: (513) 636-3723. E-mail: Bruce.Trapnell@chmcc.org.

† Present address: Department of Pediatrics, Harvard Medical School, Boston, MA 02115.

‡ Present address: Department of Laboratory Medicine, Yamagata University School of Medicine, Yamagata 990-23, Japan.

expression occurs in the absence of viral replication or late gene expression (14). Importantly, the histopathologic response is similar to that observed in Cotton rats (14, 37, 39, 60) and humans (4) and inoculation of the respiratory tract with sufficient doses of either wild-type or replication-deficient adenovirus results in significant pulmonary inflammation (14, 37). The earliest histopathological abnormality, the influx of polymorphonuclear neutrophils (PMN), is first noted 6 h after infection (37), peaks by 24 h, and evolves over the course of several days into a mononuclear cell infiltrate due to influx of both $CD4^+$ and $CD8^+$ lymphocytes and expansion of the mononuclear phagocyte pool (14, 37, 58). ARTI is accompanied by an evolving pattern of elevated levels of proinflammatory cytokines (tumor necrosis factor alpha [TNF-α], interleukin-6 [IL-6], IL-1, and interferon gamma [IFN-γ] and chemotactic chemokines (macrophage inflammatory protein-1α [MIP-1α], MIP-2, and macrophage chemotactic protein-1 [MCP-1]), the chronology of which has been partially characterized in mice over the period from 6 h to several weeks (14, 32, 37). TNF-α, IL-6, MIP-1α, and MIP-2 are among the earliest proinflammatory molecular mediators detected and are significantly elevated in lung lavage fluid at 6 h, while MCP-1, IL-1, and IFN-γ are elevated by 24 h (37). The pattern of molecular and cellular inflammation is similar in both normal and immunodeficient (athymic) mice (37), demonstrating that initiation of inflammatory signaling is independent of specific (adaptive) immunity. However, neither the precise location nor the mechanism of the initiation of inflammatory signaling during ARTI is known. Such signalling might occur in epithelial cells (which are tropic for the virus) or alveolar macrophages or as a consequence of recruited natural killer or other cells.

Alveolar macrophages (AMϕ) can provide a barrier to pulmonary infection through both intrinsic and extrinsic resistance pathways, the former by their ability to accumulate pathogenic organisms by phagocytosis and/or endocytosis and to degrade or restrict the replication of the organism and the latter by the recruitment and activation of other inflammatory cells and by their ability to act as accessory cells in adaptive immune responses (6, 53). Macrophages (Mϕ) play a central role in the acute-phase response and intrinsic resistance to some viruses, including vesicular stomatitis virus, encephalomyocarditis virus, and influenza virus, while failing to provide a barrier and instead providing a reservoir for latent infection for other viruses such as human immunodeficiency virus (reviewed in reference 53). Adenovirus is cleared from the mouse lung in a biphasic pattern consisting of an early-phase rapid elimination of approximately 60% of the adenovirus DNA within the first 24 h, followed by a late-phase slower elimination of remaining adenovirus DNA over the course of several days to weeks (56). While the late-phase elimination is known to be due to the destruction of infected epithelial cells by adenovirus-specific cytotoxic T lymphocytes (58), the very rapid onset of the early phase within the first day suggests a mechanism independent of adaptive immunity (56). This was confirmed by the finding of similar early-phase elimination kinetics in normal and immunodeficient (athymic) mice (56). Pretreatment of the lungs with clodronate-laden liposomes to deplete phagocytic cells significantly impaired early-phase clearance, suggesting that lung macrophages may mediate the rapid adenovirus clearance. However, because rapid and significant PMN influx occurs during the first 24 h of infection (37), thus overlapping the early phase of adenovirus elimination (56), PMN-mediated clearance cannot be excluded as an important mediator of viral clearance in ARTI.

The mechanism by which phagocytic cells such as AMϕ might internalize adenovirus in vivo is not known and might involve endocytosis or phagocytosis and may also involve other factors in the local milieu. The in vitro uptake of adenovirus by highly susceptible epithelial-like cells has been well studied (reviewed in reference 17), occurs by receptor-mediated endocytosis (31), and can be summarized as follows: (i) high-affinity binding of the virion to the cell mediated by attachment of the adenovirus fiber knob to its 46-kDa cell surface receptor, CAR (5); (ii) receptor clustering and rapid virion internalization via a clathrin-coated vesicle mediated by interaction of the adenovirus penton base with integrins $\alpha_v\beta_5$ or $\alpha_v\beta_3$ (28–30, 52, 54); (iii) release of clathrin to generate an endocytotic vesicle; (iv) endosome acidification mediated by an endogenous vesicular membrane proton pump (38); (v) penetration of the endosome membrane (endosome lysis) and release of the virion into the cytoplasm mediated by the TVD motif-containing cytoplasmic tail portion of integrin β_5 (51); (vi) virion translocation to the nuclear membrane mediated by microtubules (28, 45); (vii) virion binding to the nuclear pore (16); (viii) capsid disassembly at the nuclear pore (17); and (ix) translocation of viral chromatin into the nucleus through the nuclear pore (16). The ability of specific blocking agents to interrupt virion uptake at each of these sites has provided the means to study the internalization mechanism in detail (17). In contrast to highly susceptible CAR^+ cells, in vitro studies show that hematopoietic lineage cells, including AMϕ, monocytes, and related cell lines, which do not express CAR, internalize adenovirus about 100- to 1,000-fold less well (22, 23, 25, 49). Despite the very slow uptake kinetics in vitro, internalization of adenovirus by such cells in vitro requires cell surface α_v integrin, similar to CAR^+ epithelial cells, and upregulation of $\alpha_v\beta_5$ and $\alpha_v\beta_3$ on human monocytes facilitates their infection by adenovirus (22).

In this study, we hypothesized that AMϕ rapidly internalize adenovirus in vivo very early during ARTI and then directly initiate inflammatory signaling. To test this hypothesis, we examined the immediate pulmonary distribution of adenovirus and internalization by AMϕ during acute ARTI in vivo. Virion internalization was correlated with the kinetics and cellular origin of the earliest detectable stimulated proinflammatory cytokine responses. Adenovirus was very rapidly internalized by AMϕ, and the earliest detectable cytokine responses occurred in AMϕ and not airway epithelial cells as detected by in situ hybridization. To begin to define the molecular mechanism(s) whereby adenovirus stimulates inflammatory signaling in AMϕ during internalization of the virion, we correlated virion uptake with TNF-α release from adenovirus-infected macrophages after interrupting virion internalization at various sites with specific blockers. The data show that TNF-α expression in adenovirus-exposed AMϕ is initiated by a molecular mechanism activated during or subsequent to acidification of the adenovirus-containing vesicle.

MATERIALS AND METHODS

Adenovirus. The adenovirus used in this study was a human serotype 5 adenovirus carrying a 2,936-bp deletion in E1, a 1,875-bp deletion in E3, and a 3,932-bp *lacZ* marker gene within the E1 deletion (for convenience referred to as adenovirus hereafter except where otherwise specified) and has been previously described (47). For the transduction experiment, Av1GFP, an adenovirus of identical structure except expressing a mammalianized green fluorescent protein (GFP) instead of the *lacZ* marker was used. Viral growth in 293 cells, purification, and storage were done as previously described (41) except that infection was carried out in roller bottles (Falcon no. 3069) containing 12×10^7 cells/bottle and approximately five virions/cell in a Wheaton roller bottle apparatus with continuous slow rotation in a humidified atmosphere containing 5% CO_2 at 37°C. All cell culture media, medium supplements, and solutions used in virus preparation were supplied routinely or by special arrangement as endotoxin-free materials (BioWhittaker, Inc., Walkersville, Md.). Adenovirus was prepared under conditions which have previously been shown to yield undetectable levels of endotoxin using the *Limulus* amebocyte assay (BioWhittaker, Inc.) (55). The concentration of adenovirus virions was determined from the optical density

of the purified virus at 260 nm and is expressed as optical particle units (OPU) as previously described (35).

Mice. Mice (BALB/c) were maintained in a "barrier" facility in microisolation cages with filtered air under controlled ventilation and constant temperature and humidity. Bedding, food, and water were all sterilized before use, and food and water were administered ad libitum. Sterilely gowned and gloved operators performed cage changes and animal handling in a laminar flow biosafety cabinet. Sentinel mice were tested monthly to ensure a pathogen-free environment.

Localization of adenovirus within the lung after in vivo infection. To permit visualization of adenovirus virions during in vivo infection, purified adenovirus was labeled by covalent linking of the fluorescent dye, FluoroLink Cy3 (Amersham, Inc.) essentially as described by Leopold et al. (28). Virus labeling in this way results in retention of greater than 90% virus infectivity (28). A molecular sieve chromatography step using PG10 columns (Bio-Rad, Inc.) was substituted for the final dialysis step to increase the purity of the labeled virions and to eliminate traces of unlinked dye from the fluorescently labeled adenovirus (Ad-Cy3) preparations. Ad-Cy3 (4×10^{10} OPU) was administered to lungs of normal mice by transtracheal instillation (63). At subsequent times indicated in the figures, mice were anesthetized with pentobarbital and either bronchoalveolar lavage (BAL; three times with 1 ml of Hank's balanced salt solution (HBSS) containing 20 mM EDTA) was done to collect cells or the lungs were fixed in situ at 25 cm of H_2O, embedded in paraffin, and sections (5 μm) were prepared. Specimens were evaluated by fluorescence microscopy (Nikon FXTA microscope) or by confocal microscopy. Differential counts were done for cells recovered by BAL after cytocentrifugation and Diff-Quick (Dade Diagnostics, Inc.) staining as previously described (37).

Evaluation of cytokine protein levels by ELISA. Quantification of cytokine expression in murine lung following adenovirus infection was done as previously described (37). Briefly, adenovirus (4×10^{10} OPU) was administered by oral endotracheal delivery, and mice were sacrificed at various subsequent times (0.5, 3, and 6 h) by pentobarbital injection followed by exsanguination. BAL fluid was then collected as described above, cleared of cells by centrifugation ($200 \times g$, 5 min, 4°C), and stored at −80°C until use. Quantification of cytokine and chemokine levels in unconcentrated BAL fluid was accomplished by enzyme-linked immunoassay (ELISA; Quantikine M kits; R&D Systems, Minneapolis, Minn.) under conditions specified by the manufacturer.

Evaluation of cytokine mRNA expression by RT-PCR. To evaluate cytokine mRNA expression during ARTI, adenovirus (4×10^{10} OPU) was administered as described above. Mice were sacrificed at subsequent times (0.5, 3, and 6 h) as described above, and lungs were removed en bloc. Total RNA was purified by the guanidine-acid phenol-guanidinium method, subjected to reverse transcription-polymerase chain reaction (RT-PCR) amplification using cytokine gene-specific oligonucleotide primers (1), and evaluated by agarose gel electrophoresis as previously described (37). To evaluate cytokine and chemokine mRNA expression in recovered murine AMϕ, mice were infected and sacrificed as described above. AMϕ were recovered by BAL and collected by centrifugation ($200 \times g$, 5 min, 4°C), total RNA was purified with a Micro-Scale RNA Prep Kit (5 Prime-3 Prime, Inc.), and RT-PCR was carried out as described elsewhere (37).

Localization of in vivo mRNA expression by in situ hybridization. To localize expression of proinflammatory cytokine mRNA to specific cell types within the lung, mice were infected with adenovirus (4×10^{10} OPU/mouse). At subsequent times (30 min, 3 h, and 6 h), mice were sacrificed, and lung tissue was processed and evaluated by in situ hybridization with ^{35}S-labeled cRNA antisense and sense (control) probes as previously described (62). Briefly, IL-6 cRNA riboprobe synthesis was performed using a 664-bp murine IL-6 cDNA (kindly provided by Keiko Yamauchi Takihara, Osaka, Japan) subcloned into pSP72 (Promega, Inc.). TNF-α cRNA riboprobe synthesis was performed with a 1,101-bp murine TNF-α cDNA subcloned into pGEM7Z$^+$ (Promega, Inc.). Both antisense (for mRNA detection) and sense (as a control for nonspecific hybridization) [^{35}S]UTP (specific activity, 1,000 to 1,500 Ci/mmol)-labeled cRNA probes were synthesized in vitro from opposing transcriptional promoters using the Riboprobe Gemini Core System II transcription kit under conditions specified by the manufacturer (Promega, Inc.). Tissue sections were incubated at 42°C (IL-6) or 55°C (TNF-α) overnight in hybridization buffer (15 μl) containing 10^6 cpm of purified probe and 50% formamide. Following hybridization, tissues were washed to a final stringency of 0.1× SSC (1× SSC is 0.15 M NaCl plus 0.015 M sodium citrate), and autoradiography was performed using Kodak NTB2 emulsion at 4°C for periods of 3 to 8 weeks. Development was done with Kodak D19 developer as previously described (62). Representative examples of hybridization results were photographed with dark-field illumination and then counterstained with hematoxylin and eosin for bright-field or phase microscopy using a Nikon Microphot-FXA microscope.

Evaluation of adenovirus-induced cytokine induction in murine macrophages. To further explore the adenovirus-macrophage interactions that lead to induction of proinflammatory cytokine expression, in vitro studies were conducted with a murine macrophage cell line, RAW264.7 (American Type Culture Collection) (34). These cells have phagocytic properties and the capacity to secrete cytokines in response to adenovirus infection similar to that of primary AMϕ. Cells were maintained in Dulbecco modified Eagle medium (DMEM) supplemented with 10% heat-inactivated (56°C, 30 min) fetal bovine serum, 2 mM glutamine, 100 U of penicillin per ml, and 100 μg of streptomycin per ml (DMEM-10) in a humidified atmosphere containing 5% CO_2 at 37°C. The culture medium was changed every 2 to 3 days, and cells were passed using brief trypsin digestion just prior to reaching confluence. To evaluate adenovirus-stimulated macrophage TNF-α expression, cells were seeded at 10^6 cells per well in six-well plates and incubated (16 h, humidified atmosphere, 5% CO_2, 37°C). Cells were then briefly exposed to adenovirus (5×10^{10} OPU/well, 30 min), after which the medium was aspirated and replaced with DMEM-10 without virus. TNF-α release into the medium was then quantified by removing small aliquots (100 μl) of supernatant at subsequent times and quantitative determination of TNF-α concentration by ELISA. To determine at which step of adenovirus uptake TNF-α signaling is initiated, virion uptake was blocked at one of several distinct cellular sites, and then TNF-α release was quantified in supernatant 2 h after the start of infection. To evaluate the effect of blocking adenovirus internalization at the stage of phagosome closure, wortmannin, in various concentrations (0 to 300 μM) was preincubated (15 min prior to infection) with cells, followed by adenovirus infection and evaluation of TNF-α release as described above. As an additional approach to block virion entry at the cell membrane, cells were incubated at 4°C for 10 min prior to and during adenovirus infection. At subsequent times (1 to 6 h), cells were warmed to 37°C (removal of "cold block"), incubation was continued, and the TNF-α assay was done as described above. In experiments designed to evaluate the role of Ca^{2+} signaling in adenovirus-stimulated TNF-α release, cells were preincubated (30 min prior to adenovirus infection) in the absence or presence of 100 μM bis-(*o*-aminophenoxy)ethane-*N*,*N*,*N*′,*N*′-tetra-acetic acid (BAPTA) to block intracellular Ca^{2+} flux. Adenovirus infection and TNF-α expression were evaluated as described above. Chloroquine, which blocks the cellular pathway of adenovirus uptake at the endosome by blocking endosome acidification (17, 43), was used to evaluate the effect of blocking virion entry at the stage of endosome lysis. Chloroquine (50 or 100 μM) was preincubated (10 min prior to infection) with cells, followed by adenovirus exposure and evaluation of TNF-α release as above. Trypan blue exclusion was used to assess the potential for toxicity from each of the inhibitors under each of the conditions used: in every condition, cell viability was greater than 97% at the end of the experimental period (2 h after the start of infection).

Statistical method. Numerical data are presented as the mean ± the standard error of the mean. Statistical comparisons were made by using the Student's *t* test using Sigma Plot (v4.0) software on an IBM-compatible microcomputer.

RESULTS

Intrapulmonary distribution and fate of virions during early adenovirus lung infection. To directly determine the distribution and immediate fate of adenovirus following intrapulmonary administration, adenovirus labeled with the fluorescent dye, Cy3 (Ad-Cy3) was administered (4×10^{10} OPU/mouse) by tracheal instillation. Localization of Ad-Cy3 by fluorescence microscopy of unstained, paraffin-embedded sections revealed that adenovirus was rapidly and widely distributed throughout the respiratory tract (Fig. 1). Within medium and larger airways, virus was seen along the airway epithelial surfaces at approximately 1 min with little penetration into the lung parenchyma (top left panels). By 10 min, virus was observed in a punctate pattern in association with macrophages in the tissue near the terminal airways (top right panels). Fluorescence remained associated with the airway lumen and within nearby macrophages at later times (3 and 6 h; data not shown). In alveolar spaces, Ad-Cy3 was initially (~1 min) distributed predominantly in a "point-like" pattern, suggesting fine dispersion of the virions (middle left panels). By 10 min, adenovirus was found in a more punctate pattern associated with AMϕ (middle right panels). The punctate pattern of macrophage-associated fluorescence persisted at subsequent times (3 and 6 h) and became more pronounced, suggesting further accumulation in AMϕ (data not shown). Cells obtained by BAL revealed accumulation of Ad-Cy3 as early as 1 min after adenovirus instillation (bottom left panels). Accumulation was pronounced by 10 min (bottom right panels) and progressed substantially through the 6-h period of observation (30 min and 3 and 6 h; data not shown). BAL cells from adenovirus-infected mice contained greater than 95% macrophages at all times after infection up to 6 h as determined by Diff-Quick staining and differential counting ($P > 0.36$ for all comparisons of AMϕ values at 30 min, 3 h, and 6 h; Table 1). However, neutrophils were occasionally seen at 30 min and began to increase in number at 3 and 6 h (without reaching statistical significance

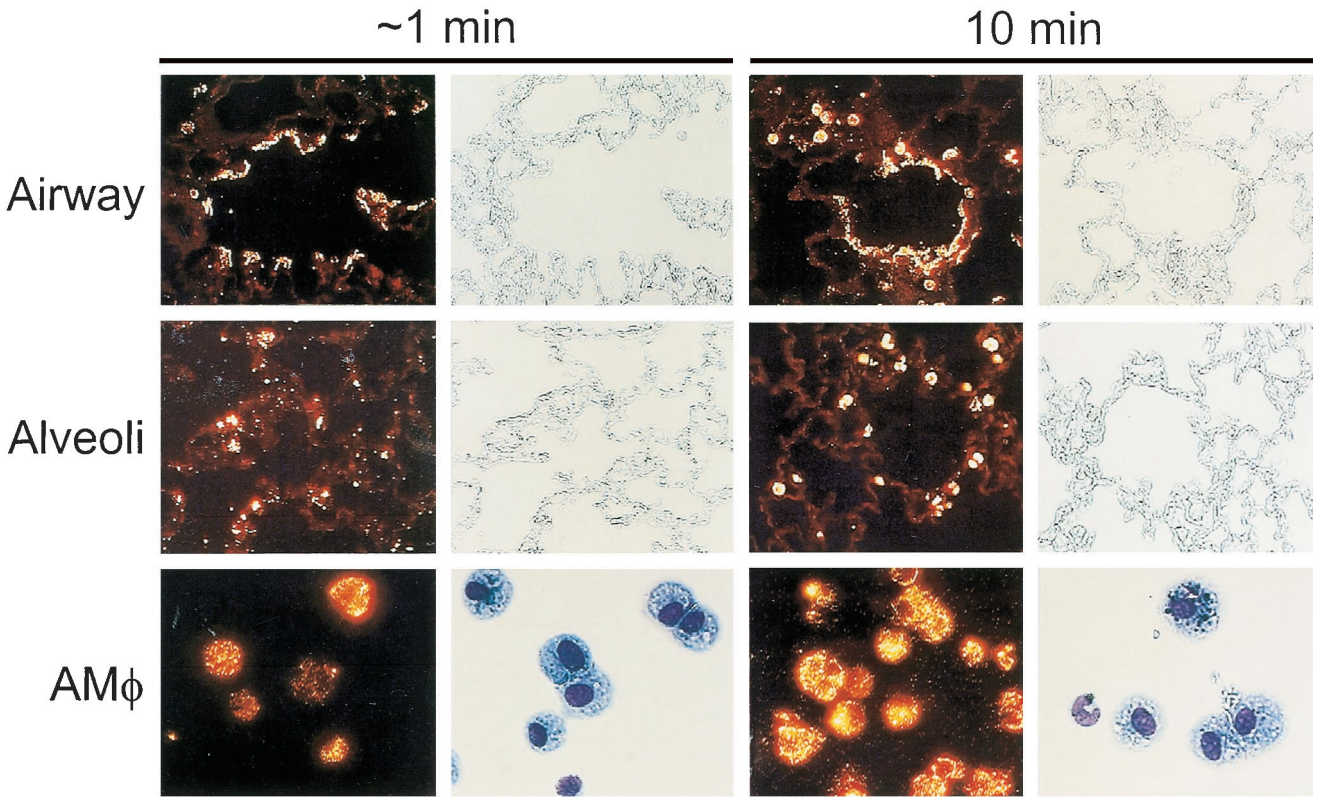

FIG. 1. Distribution of adenovirus during acute respiratory tract infection. Infectious, fluorescently labeled adenovirus (Ad-Cy3) or HBSS, as a sham control, was administered by intratracheal instillation into the lungs of mice. Mice were then sacrificed after either 1 min (left panels) or 10 min (right panels), and the lungs were removed and processed for tissue sections or the mice were subjected to BAL, followed by recovery and cytospin preparation of cells as described in Materials and Methods. Shown are fluorescence and corresponding phase photomicrographs for tissue sections (top and middle panels, ×114) and fluorescence and bright-field photomicrographs for BAL cells (bottom panels, ×232). For BAL cells, separate slides were prepared for fluorescence and bright-field photomicroscopy because Diff-Quick staining partially quenched Cy3 fluorescence.

[$P > 0.6$, all comparisons]), a result consistent with the patchy histological evidence of neutrophil infiltration at 6 h as previously observed (37). Confocal microscopy revealed the presence of Ad-Cy3 within AMϕ recovered by BAL and, interestingly, also within occasional PMN recovered at 6 h (data not shown). These data show that during ARTI in mice, adenovirus is initially widely distributed throughout the respiratory tract and that adenovirus rapidly accumulates within AMϕ.

TABLE 1. Differential cell counts for BAL cells recovered at various times from mice receiving intrapulmonary administration of adenovirus[a]

Time (h)	Administration	% Cells ± SEM		
		Macrophages	Neutrophils	Lymphocytes
0	Nothing	96.0 ± 0.5	2.2 ± 0.9	1.8 ± 0.4
0.5	Virus	97.2 ± 0.31	0.53 ± 0.29	2.3 ± 0.07
	HBSS	99.0 ± 0.30	0	1.0 ± 0.3
3	Virus	96.8 ± 1.2	2.1 ± 1.0	1.1 ± 0.24
	HBSS	99.2 ± 0.29	0.44 ± 0.29	0.33 ± 0
6	Virus	95.7 ± 1.4	3.5 ± 1.1	0.82 ± 0.32
	HBSS	98.3 ± 0.38	0.77 ± 0.28	0.9 ± 0.1

[a] Normal (BALB/c) mice ($n = 3$/group) were exposed to adenovirus and at the subsequent times indicated were sacrificed and subjected to BAL. Cells were recovered from BAL fluid by centrifugation and evaluated in cytocentrifuge preparations by routine cytological analysis. At least 200 cells were counted for each determination.

Early molecular inflammation induced by adenovirus lung infection. To identify some of the molecular mediators that initiate the cascade of pulmonary inflammation that occurs during ARTI, we measured the level of several important proinflammatory and chemotactic molecular mediators in unconcentrated BAL fluid obtained 0.5, 3, and 6 h after adenovirus administration to the lung (Fig. 2). IL-6, TNF-α, MIP-2, and MIP-1α were all significantly elevated in unconcentrated BAL fluid obtained from adenovirus-exposed mice by 6 h after infection ($P < 0.05$, all comparisons to controls; Fig. 2). TNFα, MIP-2, and MIP-1α, but not IL-6, were also elevated at 3 h. None of these cytokines were yet detectable 30 min after infection. As a sham administration control, mice exposed to HBSS did not show detectable cytokine or chemokine activity at any time (Fig. 2). To determine if adenovirus infection increased cytokine levels by stimulating gene expression, mRNA levels for these cytokines were measured in whole lung total RNA by RT-PCR as previously described (37). Cytokine mRNA transcripts were easily detected in the lungs of mice 3 and 6 h after adenovirus exposure and variably detected 30 min after adenovirus exposure (data not shown, but see below [Fig. 6] for evaluation of expression in isolated AMϕ). In contrast, mice exposed to HBSS as a sham control did not have detectable mRNA for IL-6, TNF-α, MIP-2, and MIP-1α at any time (0, 30 min, 3 h, or 6 h; data not shown). These results show that initiation of the inflammatory cascade occurs very early during

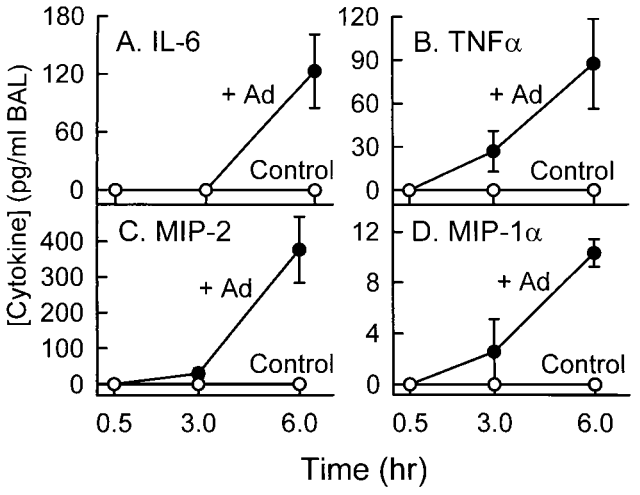

FIG. 2. Stimulation of proinflammatory cytokine and chemotactic chemokine levels in lung during acute adenovirus respiratory tract infection. Infectious adenovirus (+Ad) or HBSS (Control) was administered by intratracheal instillation into the lungs of mice (n = 3/time point). At the subsequent times indicated, mice were sacrificed and the lung epithelial lining fluid was recovered by BAL. Proinflammatory cytokine (IL-6 and TNFα) and chemoattractive chemokine (MIP-2 and MIP-1α) levels were measured in unconcentrated BAL fluid by ELISA. The entire experiment was performed twice, and representative data from one experiment are shown.

ARTI and is associated with activation of cytokine gene expression.

Localization of proinflammatory cytokine mRNA expression during early adenovirus lung infection. To determine a cell source of adenovirus-stimulated proinflammatory cytokine gene expression, expression of cytokine (IL-6, TNF-α) mRNA was evaluated by in situ hybridization. Six hours after infection, hybridization was detected in lung parenchyma with a ^{32}P-labeled IL-6 cRNA antisense probe (Fig. 3, upper left panels). As a negative control for nonspecific probe binding, a ^{32}P-labeled IL-6 cRNA sense probe did not show hybridization in lungs of virus-infected mice (upper middle panels). As a negative sham administration control, the antisense probe did not show hybridization in the lungs of mice exposed to HBSS instead of adenovirus (upper right panels). Detailed evaluation of adenovirus-infected lungs revealed intense hybridization of the IL-6 antisense probe in AMϕ (lower left panels) but not airway epithelial cells (lower middle panels) or vascular endothelial cells (lower right panels). A similar pattern of expression was observed for TNF-α 6 h after infection (Fig. 4). Specific hybridization was observed only to a ^{32}P-labeled TNF-α cRNA antisense probe in the lung parenchyma of virus-infected mice (left panels). As a negative control for nonspecific probe binding, no hybridization was observed when a ^{32}P-labeled TNF-α cRNA sense probe was incubated with lung parenchyma from virus-infected mice (middle panels) or with the antisense probe in sham HBSS administration control mice (right panels). Detailed evaluation of adenovirus-infected lung tissues showed hybridization of the TNF-α antisense probe in AMϕ but in not the airway epithelium or vascular endothelium. IL-6 and TNF-α antisense probes both showed specific hybridization to AMϕ within lung parenchyma obtained 30 min after virus administration (Fig. 5). Neither IL-6 nor TNF-α antisense probes hybridized to airway epithelium or vascular endothelium of virus-infected mice at 30 min. As negative controls for nonspecific probe binding, neither IL-6 nor TNF-α sense probes showed hybridization to lung tissues of virus-infected mice at 30 min (data not shown but similar to that presented in Fig. 3 and 4, upper middle panels). Neither IL-6 nor TNF-α antisense probes hybridized to negative sham administration controls taken at 30 min (data not shown but similar to that presented in Fig. 3 and 4, upper right panels). Similar results were obtained with these probes using lung parenchyma taken at 3 h (data not shown). These results demonstrate readily detectable expression of proinflammatory genes (e.g., IL-6 and TNF-α) by 30 min and further localize this expression to AMϕ.

Proinflammatory cytokine mRNA expression in AMϕ recovered early after adenovirus lung infection. To confirm that AMϕ were a source of stimulated expression of proinflammatory cytokines and chemotactic chemokines in the lungs of adenovirus-exposed mice, BAL cells were recovered after infection and evaluated by RT-PCR. At 3 and 6 h after adenovirus administration to the lung, IL-6, TNF-α, MIP-2, and MIP-1α mRNA transcripts were consistently detected at elevated levels in BAL cells from adenovirus-infected mice but not in sham, HBBS-exposed controls (Fig. 6). TNF-α, IL-6, MIP-2, and MIP-1α mRNA transcripts were also detectable in BAL cells recovered from virus-infected mice after only 30 min (Fig. 6). Although consistently detected at later times, at 30 min expression was variably detectable in independent experiments, suggesting that 30 min is approximately the time of the initiation of expression. Since AMϕ comprised more than 95% of the recovered BAL cells for up to 6 h after adenovirus infection in this study (Table 1), the RT-PCR data confirm that AMϕ were the likely source of the rapidly upregulated proinflammatory cytokine and chemotactic chemokine mRNA levels during ARTI. Taken together, these data demonstrate that AMϕ begin to take up adenovirus immediately after in vivo lung infection, upregulate cytokine and chemokine mRNA levels within minutes, and are the source of the earliest detectable cytokine signals in the initiation of the pulmonary inflammatory cascade during ARTI.

Mechanism of adenovirus-stimulated initiation of macrophage proinflammatory cytokine stimulation. To begin to define the molecular mechanism(s) whereby clearance of adenovirus by macrophages stimulates acute-phase, proinflammatory cytokine expression, adenovirus-stimulated TNF-α expression from the macrophage cell line, RAW264.7, was evaluated in vitro. Preliminary experiments showed that these cells were able to internalize adenovirus and rapidly responded by secretion of TNF-α with kinetics similar to those of AMϕ. Further, the in vitro approach permitted precise control of the experimental conditions required to block virion uptake into cells at various sites (17). We hypothesized that by blocking virion uptake, the molecular stimulus that initiates inflammatory cytokine signaling (e.g., TNF-α) could also be blocked. Ad-Cy3 was used to verify, by direct visualization, that adenovirus entry could be blocked at various specific cellular sites, as expected based on studies of adenovirus uptake and uncoating in epithelial cells (16, 17, 22, 23, 29, 30, 38, 43) (Fig. 7). Exposure of RAW264.7 cells to Ad-Cy3 in vitro resulted in a pattern of fluorescence demonstrating significant virus internalization, cytoplasmic translocation, and prominent extranuclear aggregation (Fig. 7A). As expected (16), incubation of virus and cells at 4°C prevented virion internalization, resulting in a pericellular rim of Ad-Cy3 fluorescence (panel C). Evaluation by confocal microscopy confirmed that virion entry into the cell was blocked at 4°C but not at 37°C (panels B and D). The intracellular calcium chelator BAPTA did not prevent virion attachment or internalization. However, little or no translocation and no significant extranuclear aggregation of fluorescence was noted in BAPTA-treated cells by either fluorescence

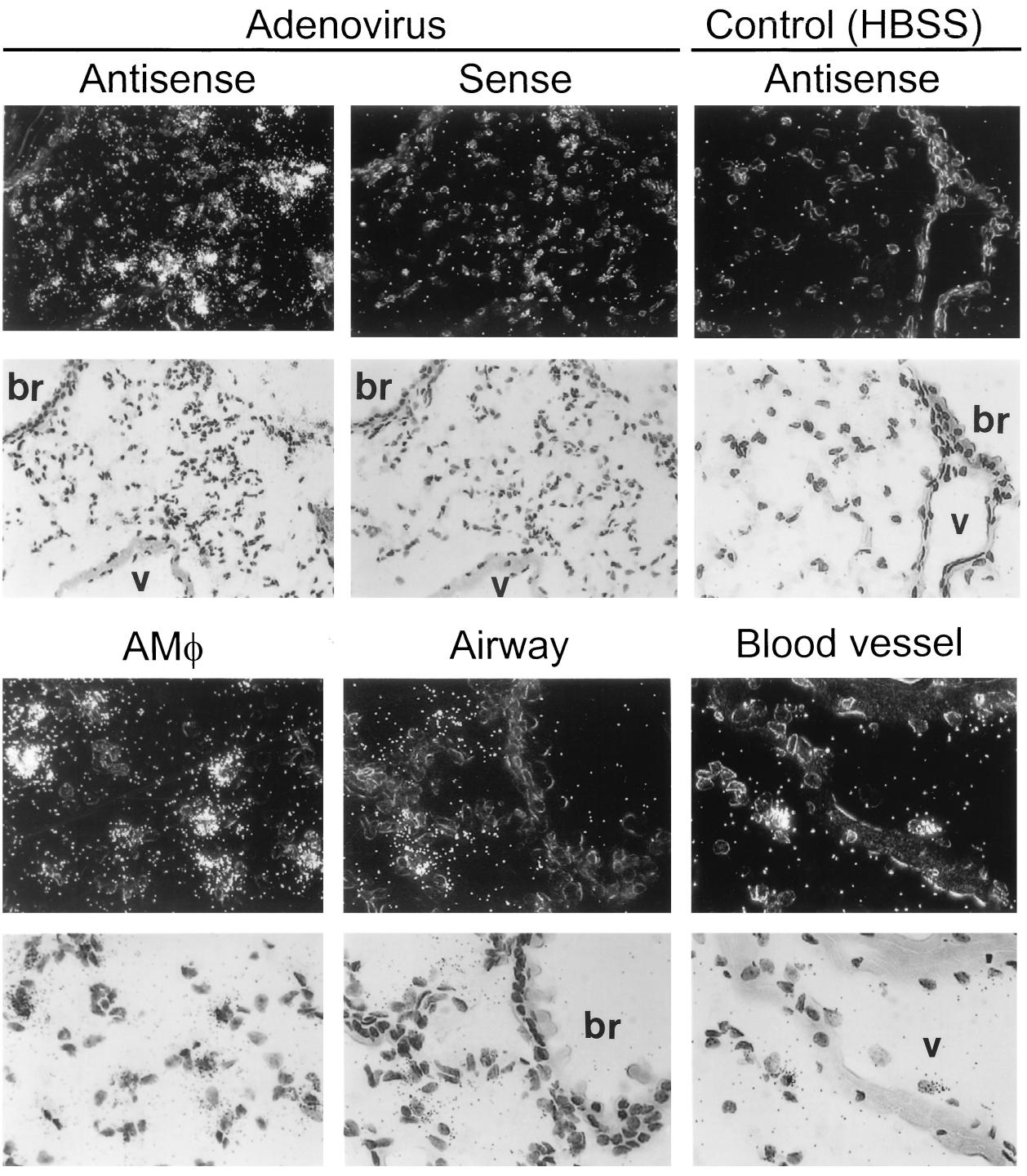

FIG. 3. Localization of IL-6 mRNA expression by in situ hybridization in lung tissues 6 h after adenovirus respiratory tract infection. Infectious adenovirus or HBSS was administered by intratracheal instillation into the lungs of mice. After 6 h, mice were sacrificed, and the lungs were removed, inflation fixed, and subjected to in situ hybridization analysis using IL-6-specific ^{35}S-labeled antisense and sense cRNA probes as described in Materials and Methods. (Upper panels) Dark-field (above) and bright-field (below) views of the hybridizations of lung tissues from adenovirus-infected or sham control (HBSS)-exposed mice with antisense or sense probes (indicated). The bronchial epithelium (br) and vascular endothelium (v) are indicated. The sense probe did not show specific hybridization in HBSS-exposed mouse lung (not shown but similar to results for sense probe [middle panels] in adenovirus-infected mice). (Left and middle panels, ×143; right panels, ×286). (Lower panels) High-power dark-field (above) and bright-field (below) views demonstrating hybridization of the antisense probe to lung tissues from adenovirus-infected mice. Bronchial and vascular tissues are indicated for upper panels (×343).

or confocal microscopy (panels E and F). As expected, wortmannin, a specific blocker of phosphatidylinositol 3-OH kinase (PI3K) (46), phagocytosis (3), and adenovirus internalization (30), did not block virion attachment to the cell surface (panels G and H), but virions were poorly internalized and did not localize as large extranuclear aggregations of fluorescence as seen in untreated cells (panels A and B). Chloroquine, which blocks endosome acidification (43) and adenovirus uptake at

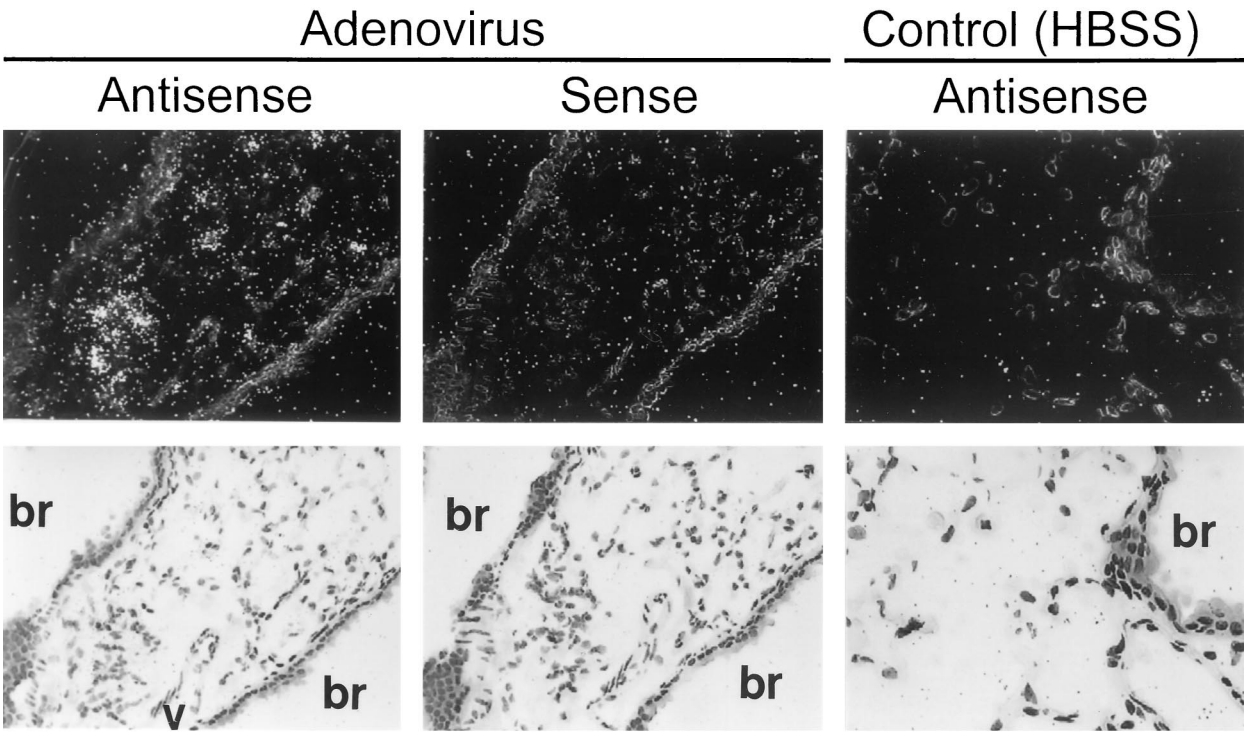

FIG. 4. Localization of TNF-α mRNA expression by in situ hybridization in lung tissues 6 h after adenovirus respiratory tract infection. Mice were exposed to adenovirus or HBSS and then sacrificed and prepared for in situ hybridization as described in the legend to Fig. 3. Tissues were hybridized with TNF-α-specific ^{35}S-labeled antisense and sense cRNA probes. Dark-field (above) and bright-field (below) views of the hybridizations of lung tissues from adenovirus-infected or sham control (HBSS)-exposed mice with antisense or sense probes (indicated) are shown. The bronchial epithelium (br) and vascular endothelium (v) are indicated. The sense probe did not show specific hybridization in HBSS-exposed mouse lung (not shown but similar to sense probe [middle panel] in adenovirus-infected mice). (Left and middle panels, ×143; right panels, ×286).

the doses used here (17), did not prevent virus attachment or internalization but did reduce the extranuclear aggregation of fluorescence (panels I and J).

To assess the fate of adenovirus in macrophages subsequent to extranuclear aggregation, we evaluated adenovirus-mediated nuclear gene transfer and expression in AMϕ, RAW264.7 macrophages and, as an epithelial-like cell positive control, A549 cells using Av1GFP. As expected, A549 cells were very efficiently transduced, and nearly all cells expressed GFP when evaluated 48 h after infection by using flow cytometry to quantify GFP-positive cells (Fig. 8, A549). In contrast, transduction of murine AMϕ was very inefficient, with only 0.2% of cells showing an increase in mean fluorescence by flow cytometry (Fig. 8, AMϕ). Similarly, RAW264.7 macrophages were also poorly transduced, with only 0.02% of cells showing an increase in mean fluorescence (Fig. 8, RAW). Evaluation of transduced cells by fluorescence microscopy demonstrated that, while nearly all A549 cells expressed GFP, none of the infected alveolar or RAW264.7 macrophages expressed GFP (data not shown). These results show that the ultimate fate of internalized adenovirus is different in macrophages and the nonphagocytic A549 cells and is consistent with inefficient nuclear delivery of the adenovirus genome in Mϕ.

To assess the mechanism of adenovirus-stimulated macrophage cytokine expression, studies were conducted using RAW264.7 macrophages infected in vitro by adenovirus in the absence or presence of various conditions known to block virion entry into cells at various sites along the pathway (17) (30). Adenovirus exposure produced a brisk, reproducible stimulation of TNF-α expression in RAW264.7 cells, resulting in easily detectable levels of TNF-α in the media at 2 h (Fig. 9; see Fig. 11 below for the time course of expression). In Ca^{2+}-free medium, adenovirus exposure resulted in marked TNF-α release at 2 h, while unexposed controls did not release any detectable TNF-α (panel A, +Ad). Results were similar in Ca^{2+}-containing medium except that TNF-α release was increased (panel B, +Ad). To investigate the role of Ca^{2+} in the mechanism of adenovirus-stimulated TNF-α expression, RAW264.7 cells were infected in the absence or presence of the intracellular Ca^{2+} chelator BAPTA. Preincubation of cells with BAPTA completely blocked TNF-α release from adenovirus-exposed cells in both Ca^{2+}-free (panel A, +BAPTA +Ad) and Ca^{2+}-containing (panel B, +BAPTA +Ad) medium. As a positive control, to demonstrate the role of extracellular Ca^{2+} influx in TNF-α expression by RAW264.7 cells, the Ca^{2+} ionophore, A23187 stimulated a large TNF-α release in Ca^{2+}-containing medium (panel B, +A23187). As a negative control for effect of this Ca^{2+} ionophore on TNF-α expression, as expected, TNF-α release did not occur in response to A23187 in Ca^{2+}-free media (panel A, +A23187). As a positive control for the blocking effects of BAPTA, the marked release of TNF-α occurring in cells exposed to a known potent TNF-α-releasing stimulus (lipopolysaccharide plus A23187) was blocked completely by BAPTA in both Ca^{2+}-free and Ca^{2+}-containing medium (+BAPTA +LPS +A23187). These observations show that adenovirus-stimulated TNF-α release by RAW264.7 macrophages is dependent on Ca^{2+} and that this flux can derive from both intra- and extracellular sources.

To determine if the signal for TNF-α release during adenovirus uptake by RAW264.7 cells occurred before or after virion

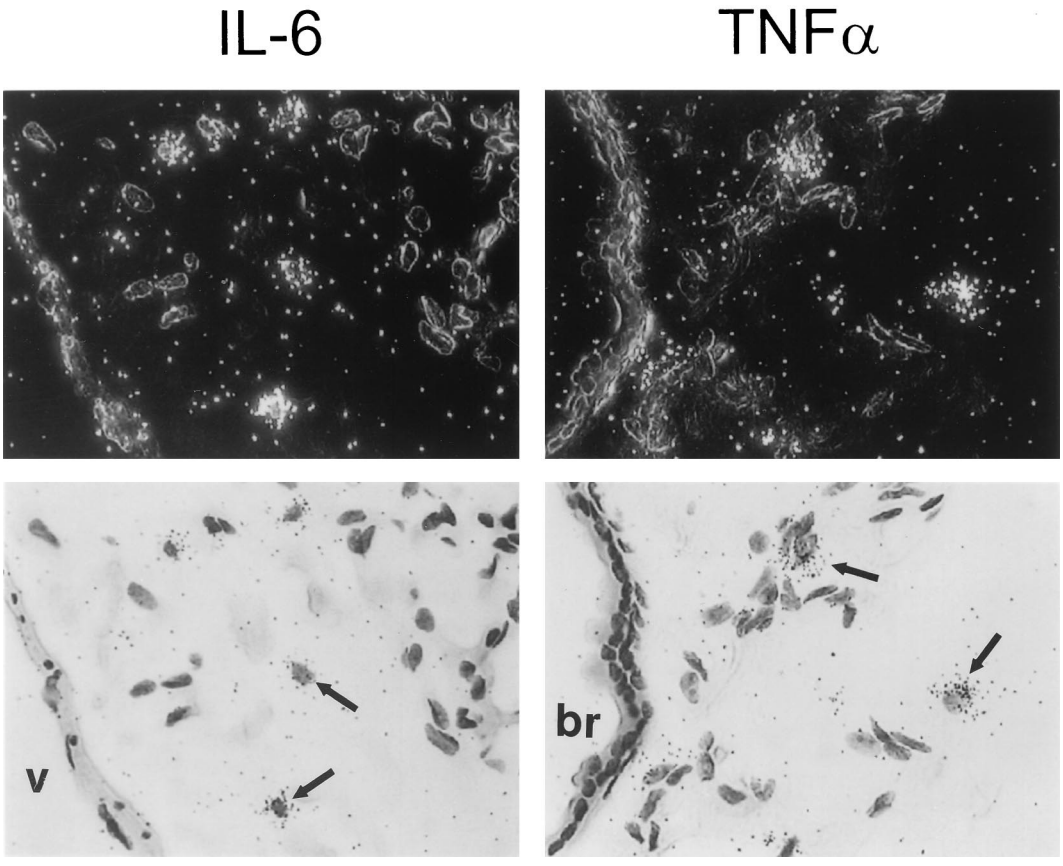

FIG. 5. Localization of IL-6 and TNF-α mRNA expression by in situ hybridization in lung tissues 30 min after adenovirus respiratory tract infection. Mice were exposed to adenovirus or HBSS and then sacrificed and prepared as described in the legend to Fig. 3 except that lung tissues were recovered 30 min after initiation of infection. In situ hybridization was done using TNF-α or IL-6-specific ^{35}S-labeled antisense or sense cRNA probes as described above. Results for mice infected with adenovirus for 30 min after hybridization to antisense probes for IL-6 (left panels) or TNF-α (right panels) are shown. For each field, both dark-field (above) and bright-field (below) views are shown. Note the hybridization in AMϕ (arrows) but not in the bronchial (br) epithelium or the vascular (v) endothelium. The results for the sense probe and HBSS sham infection controls are shown in Fig. 3 and 4 (experiments conducted simultaneously). Magnification, ×430.

internalization, wortmannin was used to block virion internalization (Fig. 7D). Wortmannin blocked adenovirus-stimulated TNF-α release in a dose-dependent manner (Fig. 10). To further assess virion internalization in the mechanism of adenovirus-stimulated TNF-α release by macrophages, cold-induced blockade of virion uptake was evaluated (17). Incubation of virus with cells at 4°C blocked virion internalization, but not cell binding (Fig. 7B) as previously described (17), and completely blocked TNF-α expression for the duration of the experiment (data not shown). When cells were allowed to bind adenovirus at 4°C and subsequently (after 1, 2, 3, and 6 h) warmed to 37°C, TNF-α release was delayed by an amount related to the time of the shift to 37°C and not the total time from the start virus exposure (data not shown). Thus, TNF-α release by adenovirus-exposed macrophages was correlated with virion internalization, and virion binding to the cell surface in

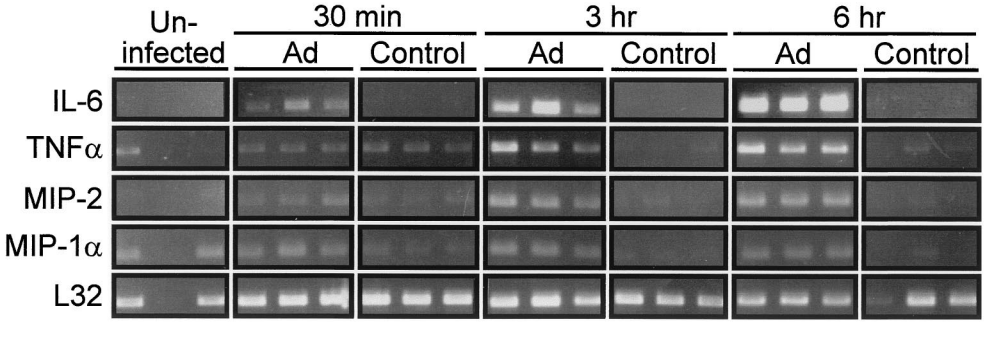

FIG. 6. Stimulation of proinflammatory cytokine mRNA levels in AMϕ recovered after adenovirus respiratory tract infection. Mice were exposed to adenovirus (Ad) or HBSS (Control) and sacrificed at subsequent times (indicated), and RT-PCR analysis was done as described in Materials and Methods. All experiments were conducted twice and results from experiment 1 (IL-6) or experiment 2 (TNF-α, MIP-2, MIP-1α, and L32) were chosen so as to permit adequate photographic reproduction of the data at 30 min. Each lane represents data from a separate mouse.

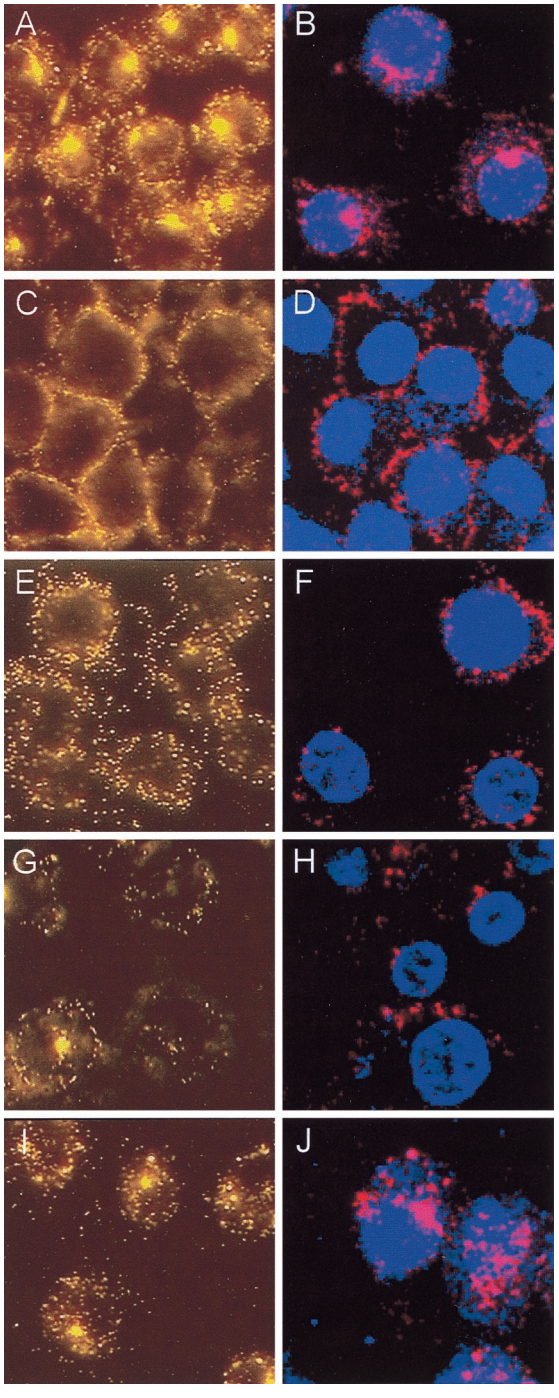

FIG. 7. Direct visualization of uptake of adenovirus virions by cultured macrophages in vitro and blockage of uptake at distinct stages. Ad-Cy3 was incubated with RAW264.7 cells under various conditions, and the results were evaluated by fluorescence (A, C, E, G, and I) and confocal (B, D, F, H, and J) microscopy as described in Materials and Methods. (A and B) Infection at 37°C. (C and D) Infection at 4°C. (E and F) Effect of the Ca^{2+} chelator, BAPTA, on the cellular distribution of virions during infection at 37°C. (G and H) Effect of wortmannin, a PI3K inhibitor known to block adenovirus endocytosis. (I and J) Effect of chloroquine, a lysosomotropic agent know to block endosome acidification. All panels, ×706.

the absence of internalization was insufficient for TNFα release. Together, these observations show that TNF-α release is initiated by a molecular mechanism subsequent to internalization of the virion into the cell, but not by virion binding to the cell alone.

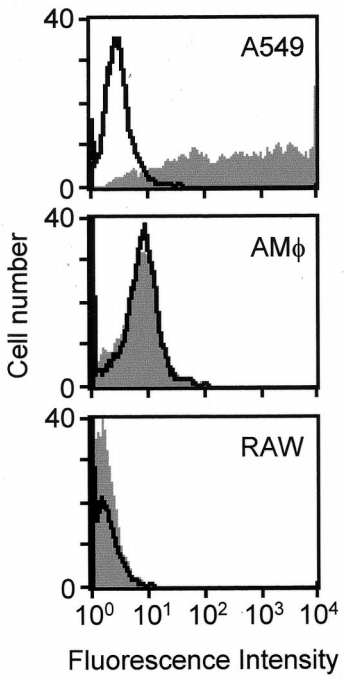

FIG. 8. Analysis of adenovirus-mediated transgene delivery and expression. AMϕ, RAW264.7 macrophages, or A549 cells, as an epithelial-like cell positive control, were infected with Av1GFP, an adenovirus vector similar in structure to Av1nBg except expressing a mammalianized GFP encoding transgene. After 48 h, cells were evaluated for GFP expression by quantifying fluorescence using flow cytometry (gray profiles). Uninfected control cell samples were also evaluated (black profiles).

To determine if the initiation of TNF-α release occurs before or after endosome acidification, cells were incubated in the absence or presence of chloroquine under conditions known to block endosome acidification (17, 43). Chloroquine completely blocked adenovirus-stimulated TNF-α release at two different doses (50 and 100 μM) (Fig. 11).

Taken together, these data suggest that the signal for initiation of TNF-α expression during adenovirus exposure to macrophages requires virion internalization, likely occurs during or subsequent to endosome acidification, and is calcium dependent.

DISCUSSION

In the current study, we sought to obtain information regarding the mechanism of initiation of the pulmonary inflammatory signaling during adenovirus respiratory tract infection. Our results demonstrate that adenovirus is rapidly distributed throughout the mouse lung and is also very quickly internalized by alveolar macrophages in vivo. Concurrently, inflammatory cytokine signaling is initiated in AMϕ but not in airway epithelial or vascular endothelial cells. Finally, the mechanism of macrophage-mediated TNF release requires internalization of the virion and is calcium dependent.

An important focus of these studies was the determination of the in vivo fate of adenovirus during ARTI. Adenovirus was already widely distributed throughout airway and alveolar epithelial surfaces following intratracheal instillation at the earliest times feasible for direct evaluation and was rapidly taken up by AMϕ. This very rapid in vivo uptake of adenovirus by AMϕ is surprising for several reasons. First, AMϕ and other hematopoietic lineage cells do not express the high-affinity adenovirus receptor CAR (22, 23, 25, 49), and thus in vitro

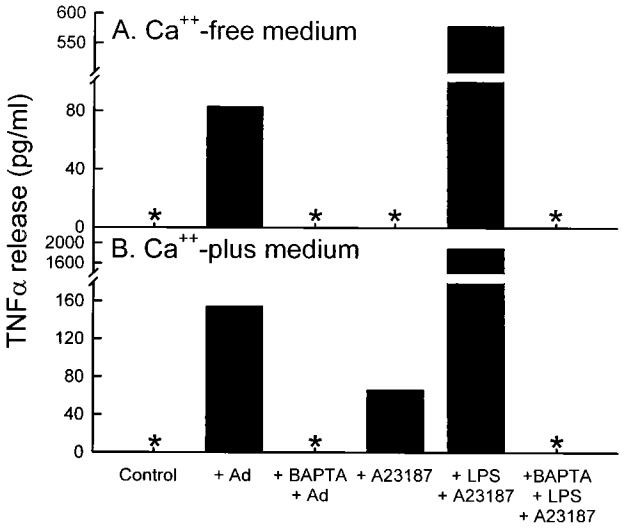

FIG. 9. Adenovirus-stimulated macrophage TNF-α expression in vitro does not occur in the presence of the Ca^{2+} chelator, BAPTA. RAW264.7 cells were evaluated for TNF-α expression and release 2 h after a 30-min in vitro exposure to adenovirus. All experiments were carried out in the absence (A) or presence (B) of Ca^{2+} in the culture medium. Cells were infected with adenovirus alone (+Ad) or in the presence of the intracellular Ca^{2+} chelator, BAPTA (+BAPTA +Ad) to demonstrate the effect of blocking intracellular calcium fluxes on adenovirus-stimulated TNF-α expression. Cells were exposed to HBSS (Control) alone as a negative control for spontaneous TNF-α release. Cells were treated with the calcium ionophore, A23187 in Ca^{2+}-free or Ca^{2+}-containing medium as controls to demonstrate the role of the extracellular Ca^{2+} in stimulation of TNF-α expression in RAW264.7 cells. As an additional positive control, cells were exposed to lipopolysaccharide and A23187 (+ LPS + A23187), a potent stimulus for TNF-α expression in RAW264.7 cells. As an additional control to demonstrate the blocking effect of BAPTA, LPS-A23187 stimulation was done in the presence of BAPTA (+BAPTA +LPS +A23187).

virion binding is reduced ca. 100-fold compared to CAR^+ cells (9). Reintroduction of CAR into AMϕ significantly increased adenovirus binding and the rate of infection in vitro (25). Second, monocytes and monocytic cell lines express the coreceptor, $\alpha_v\beta_5$ integrin, at low levels, thus reducing adenovirus internalization (22). Third, the rate of adenovirus infection in vitro is slow even in highly susceptible cells that express CAR due to the rate-limiting step of extracellular diffusion of virions to the cell surface (35). Taken together, these observations suggest the possibility that an additional factor may accelerate internalization of adenovirus by AMϕ in vivo. There are multiple candidates for such a factor, including complement proteins or natural antibodies, which are important in the uptake of some viruses (53), and collectins such as surfactant proteins A and D, which are involved in lung host defense (11). Such a role for surfactant proteins is supported by data from mice genetically deficient in surfactant protein A expression that show reduced in vivo adenovirus uptake by AMϕ during ARTI (19). Interactions between surfactant and adenovirus are also supported by data showing that coadministration of surfactant with an adenovirus vector expressing a marker gene resulted in a wider distribution of infection and gene transfer within the lungs of rabbits (24). In vivo uptake and internalization adenovirus by AMϕ may also be facilitated by the expression of $\alpha_v\beta_5$ integrins because adenovirus uptake into most, if not all, other cells, including monocytes, requires $\alpha_v\beta_5$ or $\alpha_v\beta_3$ integrin, and upregulation of $\alpha_v\beta_5$ integrin expression on monocytes correspondingly increases their rate of infection by adenovirus in vitro (22). The precise mechanism of virion uptake by AMϕ in vivo is not known and may involve endocytosis, phagocytosis, or both; further studies are needed to determine the mechanism.

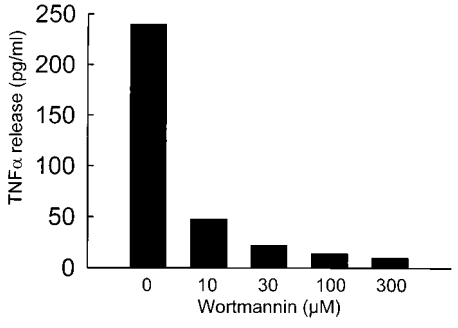

FIG. 10. Adenovirus-stimulated macrophage TNF-α expression does not occur when virion internalization is blocked by wortmannin. RAW264.7 cells were infected by adenovirus in vitro in the absence or presence of various concentrations of the PI3K inhibitor, wortmannin, and TNF-α expression was measured at 2 h as described in Materials and Methods.

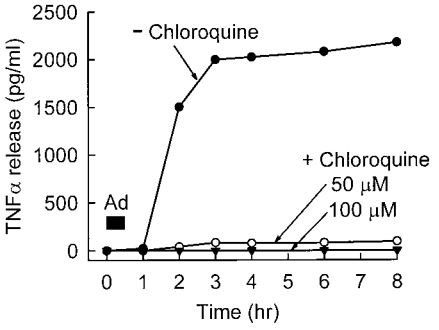

FIG. 11. Adenovirus-stimulated macrophage TNF-α expression does not occur when endosome acidification is blocked by chloroquine. RAW264.7 cells were infected by adenovirus in vitro in the absence or presence of two concentrations of chloroquine to block endosome-lysosome acidification, and TNF-α release into the culture medium was measured at various subsequent times as described in Materials and Methods.

Our results are consistent with earlier studies (56) that proposed a role for AMϕ in the clearance of adenovirus from the lung. However, a role for PMN-mediated adenovirus uptake and clearance from the lung has not been excluded. Importantly, our direct observations using confocal microscopy demonstrated that AMϕ and PMN both internalize adenovirus during ARTI. Thus, further studies will be required to determine the relative contributions of AMϕ and newly recruited PMN in the clearance of adenovirus from the lung. Very little (<5%) of the internalized adenovirus is eliminated by lysosomal degradation in highly susceptible cells (e.g., epithelial cells) (17, 56). In contrast, AMϕ degrade a large proportion of adenovirus administered in vivo (56). Further, although AMϕ rapidly can internalize adenovirus in vivo, they are transduced with very low efficiency. Thus, the pathway and fate of adenovirus in AMϕ and epithelial cells appears to be fundamentally different or a common pathway may diverge at a point after endosome formation. Alternative pathways for adenovirus infection have been shown in fibroblasts in the absence or presence of CAR expression (20). The notion that AMϕ efficiently degrade adenovirus is not supported by data showing that adenovirus can persistently infect hematopoietic lineage cells, including monocytes, thus providing a reservoir for latent infection (2, 9). Also inconsistent is the finding that AMϕ can

harbor replication-deficient adenovirus vectors for up to 5 weeks in immunocompetent mice in vivo (57).

The major focus of the present study was to obtain information regarding the mechanism of activation of the pulmonary inflammatory signaling during ARTI. The sequence of inflammatory events at late times following adenovirus infection of the lung has been best studied in animal models and consists of an evolving cascade of molecular and cellular mediators (14, 37, 44, 55, 58, 60, 63). In mice, cellular infiltration by PMN is noted in the lung as early as 6 h after adenovirus administration (37). This increases in magnitude, eventually giving way to a predominantly mononuclear cell infiltrate over the course of several days. Elevated levels of several proinflammatory cytokines and chemokines have also been observed at intermediate times during ARTI. For example, elevated lung cytokine levels were detected during ARTI for TNF-α, IL-6, MIP-1α, and MIP-2 in mice (37), IL-8 in nonhuman primates (55), and IL-6 in humans (33). In humans, exposure of the adenovirus to AMϕ was postulated as the cause of elevated IL-6 levels (33). Consistent with this concept, following reduction of the volume of adenovirus inoculum to prevent alveolar spread of virus (thus reducing exposure to AMϕ), subsequently treated patients did not show elevated IL-6 levels (33). In the present study, TNF-α was detectable 3 h after adenovirus infection, and IL-6 was detectable at 6 h. Importantly, in situ hybridization demonstrated elevated mRNA levels for both cytokines in macrophages at 30 min, suggesting a common, very early activation signal. NF-κB could provide such a signaling mechanism, and this factor has been reported to be required for stimulation of TNF-α expression in AMϕ (27). Nonetheless, no mRNA expression for either cytokine was observed in airway or vascular endothelia, thus clearly identifying AMϕ as the site of initiation of the pulmonary inflammatory cytokine cascade. Our results are consistent with in vitro data that showed that cultured human bronchial epithelial cells do not secrete cytokines after adenovirus exposure even though TNF-α, as a positive control, stimulated IL-6 and IL-8 expression (36).

Several lines of evidence suggest that inflammation during ARTI is initiated within AMϕ during virion uptake and/or degradation rather than as a response of natural killer or other cells to infected epithelial cells or by events within epithelial or vascular cells. In vivo, adenovirus infection increased levels of TNF-α mRNA in AMϕ by 30 min and protein in BAL by 3 h. RAW264.7 macrophages infected at high multiplicity in vitro showed similar TNF-α expression kinetics and demonstrated that macrophages alone are sufficient for initiation of cytokine signaling. Further, TNF-α expression was completely abrogated when virion internalization was interrupted at one of several distinct cellular sites. Previous studies have demonstrated that receptor-mediated adenovirus internalization by epithelial cells is blocked by wortmannin or infection at 4°C (17, 30). Both of these conditions completely blocked adenovirus internalization and TNF-α expression. Blocking intracellular Ca^{2+} flux completely abrogated TNF-α expression by RAW264.7 cells. Although BAPTA did not affect virion internalization, it prevented late extranuclear aggregation of adenovirus. Ca^{2+} is known to be involved in adenovirus uptake in CAR-expressing epithelial cells at early and late times (16). Although the precise point of the early involvement is not known, the later involvement occurs during virion binding to the nuclear pore (16). It is interesting that BAPTA enhanced adenovirus-mediated gene transfer to airway epithelium during in vivo administration to the lung (50). This enhancement was attributed to an effect on airway cell tight junction permeability, although potential effects on macrophage virion uptake were not evaluated. Chloroquine, at the doses used here, has been shown to block endosome-lysosome acidification (38) and also adenovirus-mediated endosome lysis and cellular infection (17). At lower doses (5 to 10 μM) which reduce the toxicity seen at late times (48 to 72 h) after infection, chloroquine was reported to block endosome acidification but did not affect adenovirus infection of HeLa cells (40). Our data demonstrated that chloroquine completely blocked TNF-α expression in RAW264.7 macrophages and appears to have altered the intracellular distribution of adenovirus, reducing the extranuclear aggregation. Our results with chloroquine and the various inhibitors in these short-term experiments cannot be explained on the basis of toxicity since >97% of cells were viable under all conditions evaluated as determined by trypan blue exclusion. Expression of adenoviral early genes such as those of the E1 region has been postulated as important in stimulating the inflammatory cascade during ARTI in the mouse model (15). The adenovirus mutant used here was devoid of E1 genes and also E3 region genes known to modulate inflammatory responses (18) but still rapidly initiated inflammation during ARTI. Thus, our data do not support a requirement for adenovirus early gene expression in the initiation of pulmonary inflammation. Taken together, our data suggest that the molecular event that initiates cytokine gene expression in AMϕ during virus clearance occurs during or subsequent to endosome acidification.

These observations have implications for the development of adenovirus vectors for human gene therapy for cystic fibrosis and lung disorders. Inflammation has been observed in multiple clinical trials where replication-deficient adenovirus vectors have been administered to the respiratory tract (7). Importantly, inflammation occurred after vector administration to nasal and bronchial epithelium. Thus, vector delivery to the alveolar surface cannot completely explain the inflammatory host response as previously proposed (33). Nasal inflammatory responses to adenovirus appear not to be explained by an epithelial cell response because cultured primary airway epithelial cells do not stimulate cytokines following in vitro adenovirus infection (36). These prior findings may be reconciled by the fact that macrophages are found on the epithelial surface distributed throughout the respiratory tract with a density in proportion to the surface area (6, 10) and our observations that macrophages initiate the inflammatory response during adenovirus infection.

ACKNOWLEDGMENTS

We thank Keiko Takihara for the generous gift of the murine IL-6 cDNA, Kim Wilmer for help with animal husbandry, and Jeff Whitsett for critical reading of the manuscript.

This work was supported by the Cystic Fibrosis Foundation (S887) and the Children's Hospital Research Foundation, Cincinnati, Ohio.

REFERENCES

1. **Allen, R. D., T. A. Staley, and C. L. Sidman.** 1993. Differential cytokine expression in acute and chronic murine graft- versus-host-disease. Eur. J. Immunol. **23:**333–337.
2. **Andiman, W. A., and G. Miller.** 1982. Persistent infection with adenovirus types 5 and 6 in lymphoid cells from humans and woolly monkeys. J. Infect. Dis. **145:**83–88.
3. **Araki, N., M. T. Johnson, and J. A. Swanson.** 1996. A role for phosphoinositide 3-OH kinase in the completion of macropinocytosis and phagocytosis by macrophages. J. Cell Biol. **135:**1249–1260.
4. **Becroft, D. M.** 1967. Histopathology of fatal adenovirus infection of the respiratory tract in young children. J. Clin. Pathol. **20:**561–569.
5. **Bergelson, J. M., A. Krithivas, L. Celi, G. Droguett, M. S. Horwitz, T. Wickham, R. L. Crowell, and R. W. Finberg.** 1998. The murine CAR homolog is a receptor for coxsackie B viruses and adenoviruses. J. Virol. **72:**415–419.
6. **Bezdicek, P., and R. G. Crystal.** 1997. Pulmonary macrophages, p. 859–875. *In* R. G. Crystal, P. J. Barnes, J. B. West, and E. R. Weibel (ed.), The lung:

scientific foundations, 2nd ed., vol. 1. Lippincott-Raven, Philadelphia, Pa.
7. **Boucher, R. C.** 1999. Status of gene therapy for cystic fibrosis lung disease. J. Clin. Investig. **103:**441–445.
8. **Brody, S. L., M. Metzger, C. Danel, M. A. Rosenfeld, and R. G. Crystal.** 1994. Acute responses of non-human primates to airway delivery of an adenovirus vector containing the human cystic fibrosis transmembrane conductance regulator cDNA. Hum. Gene Ther. **5:**821–836.
9. **Chu, Y., K. Sperber, L. Mayer, and M. T. Hsu.** 1992. Persistent infection of human adenovirus type 5 in human monocyte cell lines. Virology **188:**793–800.
10. **Crapo, J. D., B. E. Barry, P. Gehr, M. Bachofen, and E. R. Weibel.** 1982. Cell number and cell characteristics of the normal human lung. Am. Rev. Respir. Dis. **126:**332–337.
11. **Crouch, E. C.** 1998. Collectins and pulmonary host defense. Am. J. Respir. Cell Mol. Biol. **19:**177–201.
12. **Crystal, R. G., N. G. McElvaney, M. A. Rosenfeld, C. S. Chu, A. Mastrangeli, J. G. Hay, S. L. Brody, H. A. Jaffe, N. T. Eissa, and C. Danel.** 1994. Administration of an adenovirus containing the human CFTR cDNA to the respiratory tract of individuals with cystic fibrosis. Nat. Genet. **8:**42–51.
13. **Fraser, R. S., N. L. Muller, N. Colman, and P. D. Pare.** 1999. Viral respiratory diseases, p. 994–996. *In* R. S. Fraser and P. D. Pare's (ed.), Diagnosis of diseases of the chest, 4th ed., vol. 2. W. B. Saunders Co., Philadelphia, Pa.
14. **Ginsberg, H. S., L. L. Moldawer, P. B. Sehgal, M. Redington, P. L. Kilian, R. M. Chanock, and G. A. Prince.** 1991. A mouse model for investigating the molecular pathogenesis of adenovirus pneumonia. Proc. Natl. Acad. Sci. USA **88:**1651–1655.
15. **Ginsberg, H. S., and G. A. Prince.** 1994. The molecular basis of adenovirus pathogenesis. Infect. Agents Dis. **3:**1–8.
16. **Greber, U. F., M. Suomalainen, R. P. Stidwill, K. Boucke, M. W. Ebersold, and A. Helenius.** 1997. The role of the nuclear pore complex in adenovirus DNA entry. EMBO J. **16:**5998–6007.
17. **Greber, U. F., M. Willetts, P. Webster, and A. Helenius.** 1993. Stepwise dismantling of adenovirus 2 during entry into cells. Cell **75:**477–486.
18. **Harrod, K. S., T. W. Hermiston, B. C. Trapnell, W. S. Wold, and J. A. Whitsett.** 1998. Lung-specific expression of adenovirus E3-14.7K in transgenic mice attenuates adenoviral vector-mediated lung inflammation and enhances transgene expression. Hum. Gene Ther. **9:**1885–1898.
19. **Harrod, K. S., B. C. Trapnell, K. Otake, T. R. Korfhagen, and J. A. Whitsett.** 1999. SP-A enhances viral clearance and inhibits inflammation after pulmonary adenoviral infection. Am. J. Physiol. **277:**L580–L588.
20. **Hidaka, C., E. Milano, P. L. Leopold, J. M. Bergelson, N. R. Hackett, R. W. Finberg, T. J. Wickham, I. Kovesdi, P. Roelvink, and R. G. Crystal.** 1999. CAR-dependent and CAR-independent pathways of adenovirus vector-mediated gene transfer and expression in human fibroblasts. J. Clin. Investig. **103:**579–587.
21. **Horowitz, M. S.** 1996. Adenoviruses, p. 2149–2171. *In* B. N. Fields, D. M. Knipe, and P. M. Howley (ed.), Fields virology, 3rd ed., vol. 2. Lippincott-Raven Publishers, New York, N.Y.
22. **Huang, S., R. I. Endo, and G. R. Nemerow.** 1995. Upregulation of integrins $\alpha_v\beta_3$ and $\alpha_v\beta_5$ on human monocytes and T lymphocytes facilitates adenovirus-mediated gene delivery. J. Virol. **69:**2257–2263.
23. **Huang, S., T. Kamata, Y. Takada, Z. M. Ruggeri, and G. R. Nemerow.** 1996. Adenovirus interaction with distinct integrins mediates separate events in cell entry and gene delivery to hematopoietic cells. J. Virol. **70:**4502–4508.
24. **Jobe, A. H., T. Ueda, J. A. Whitsett, B. C. Trapnell, and M. Ikegami.** 1996. Surfactant enhances adenovirus-mediated gene expression in rabbit lungs. Gene Ther. **3:**775–779.
25. **Kaner, R. J., S. Worgall, P. L. Leopold, E. Stolze, E. Milano, C. Hidaka, R. Ramalingam, N. R. Hackett, R. Singh, J. Bergelson, R. Finberg, E. Falck-Pedersen, and R. G. Crystal.** 1999. Modification of the genetic program of human alveolar macrophages by adenovirus vectors in vitro is feasible but inefficient, limited in part by the low level of expression of the coxsackie/adenovirus receptor. Am. J. Respir. Cell Mol. Biol. **20:**361–370.
26. **Knowles, M. R., K. W. Hohneker, Z. Zhou, J. C. Olsen, T. L. Noah, P. C. Hu, M. W. Leigh, J. F. Engelhardt, L. J. Edwards, K. R. Jones, et al.** 1995. A controlled study of adenoviral-vector-mediated gene transfer in the nasal epithelium of patients with cystic fibrosis. N. Engl. J. Med. **333:**823–831.
27. **Lentsch, A. B., B. J. Czermak, N. M. Bless, N. Van Rooijen, and P. A. Ward.** 1999. Essential role of alveolar macrophages in intrapulmonary activation of NF-kappaB. Am. J. Respir. Cell Mol. Biol. **20:**692–698.
28. **Leopold, P. L., B. Ferris, I. Grinberg, S. Worgall, N. R. Hackett, and R. G. Crystal.** 1998. Fluorescent virions: dynamic tracking of the pathway of adenoviral gene transfer vectors in living cells. Hum. Gene Ther. **9:**367–378.
29. **Li, E., D. Stupack, G. M. Bokoch, and G. R. Nemerow.** 1998. Adenovirus endocytosis requires actin cytoskeleton reorganization mediated by Rho family GTPases. J. Virol. **72:**8806–8812.
30. **Li, E., D. Stupack, R. Klemke, D. A. Cheresh, and G. R. Nemerow.** 1998. Adenovirus endocytosis via α_v integrins requires phosphoinositide-3-OH kinase. J. Virol. **72:**2055–2061.
31. **Marsh, M., and H. T. McMahon.** 1999. The structural era of endocytosis. Science **285:**215–220.
32. **McCoy, R. D., B. L. Davidson, B. J. Roessler, G. B. Huffnagle, S. L. Janich, T. J. Laing, and R. H. Simon.** 1995. Pulmonary inflammation induced by incomplete or inactivated adenoviral particles. Hum. Gene Ther. **6:**1553–1560.
33. **McElvaney, N. G., and R. G. Crystal.** 1995. IL-6 release and airway administration of human CFR cDNA adenovirus vector. Nat. Med. **1:**182–184.
34. **McKernan, L. N., and M. T. Largen.** 1983. Identification of multiple-molecular-weight forms of thymocyte comitogenic activity from the monocyte/macrophage cell line RAW 264.7. Cell. Immunol. **80:**84–96.
35. **Mittereder, N., K. L. March, and B. C. Trapnell.** 1996. Evaluation of the concentration and bioactivity of adenovirus vectors for gene therapy. J. Virol. **70:**7498–7509.
36. **Noah, T. L., I. A. Wortman, P. C. Hu, M. W. Leigh, and R. C. Boucher.** 1996. Cytokine production by cultured human bronchial epithelial cells infected with a replication-deficient adenoviral gene transfer vector or wild-type adenovirus type 5. Am. J. Respir. Cell Mol. Biol. **14:**417–424.
37. **Otake, K., D. L. Ennist, K. Harrod, and B. C. Trapnell.** 1998. Nonspecific inflammation inhibits adenovirus-mediated pulmonary gene transfer and expression independent of specific acquired immune responses. Hum. Gene Ther. **9:**2207–2222.
38. **Perez, L., and L. Carrasco.** 1994. Involvement of the vacuolar $H^{(+)}$-ATPase in animal virus entry. J. Gen. Virol. **75:**2595–606.
39. **Prince, G. A., D. D. Porter, A. B. Jenson, R. L. Horswood, R. M. Chanock, and H. S. Ginsberg.** 1993. Pathogenesis of adenovirus type 5 pneumonia in cotton rats (*Sigmodon hispidus*). J. Virol. **67:**101–111.
40. **Rodriguez, E., and E. Everitt.** 1996. Adenovirus uncoating and nuclear establishment are not affected by weak base amines. J. Virol. **70:**3470–3477.
41. **Rosenfeld, M. A., K. Yoshimura, B. C. Trapnell, K. Yoneyama, E. R. Rosenthal, W. Dalemans, M. Fukayama, J. Bargon, L. E. Stier, L. Stratford-Perricaudet, et al.** 1992. In vivo transfer of the human cystic fibrosis transmembrane conductance regulator gene to the airway epithelium. Cell **68:**143–155.
42. **Rubin, B. A., and L. B. Rorke.** 1988. Adenovirus vaccines, p. 492–512. *In* S. A. Plotkin and J. Y. Mortimer (ed.), Vaccines. W. B. Saunders, Philadelphia, Pa.
43. **Seglen, P. O., B. Grinde, and A. E. Solheim.** 1979. Inhibition of the lysosomal pathway of protein degradation in isolated rat hepatocytes by ammonia, methylamine, chloroquine and leupeptin. Eur. J. Biochem. **95:**215–225.
44. **Simon, R. H., J. F. Engelhardt, Y. Yang, M. Zepeda, S. Weber-Pendleton, M. Grossman, and J. M. Wilson.** 1993. Adenovirus-mediated transfer of the CFTR gene to lung of nonhuman primates: toxicity study. Hum. Gene Ther. **4:**771–780.
45. **Suomalainen, M., M. Y. Nakano, S. Keller, K. Boucke, R. P. Stidwill, and U. F. Greber.** 1999. Microtubule-dependent plus and minus end-directed motilities are competing processes for nuclear targeting of adenovirus. J. Cell Biol. **144:**657–672.
46. **Swanson, J. A., M. T. Johnson, K. Beningo, P. Post, M. Mooseker, and N. Araki.** 1999. A contractile activity that closes phagosomes in macrophages. J. Cell Sci. **112:**307–316.
47. **Trapnell, B. C.** 1993. Adenoviral vectors for gene transfer. Adv. Drug Delivery Rev. **12:**185–199.
48. **Trapnell, B. C.** 1997. Gene therapy for cystic fibrosis lung disease. *In* R. W. Wilmott (ed.), The pediatric lung. Birkhauser Verlag, Basel, Switzerland.
49. **Von Seggern, D. J., C. Y. Chiu, S. K. Fleck, P. L. Stewart, and G. R. Nemerow.** 1999. A helper-independent adenovirus vector with E1, E3, and fiber deleted: structure and infectivity of fiberless particles. J. Virol. **73:**1601–1608.
50. **Wang, G., J. Zabner, C. Deering, J. Launspach, J. Shao, M. Bodner, D. J. Jolly, B. L. Davidson, and P. McCray.** 2000. Increasing epithelial junction permeability enhances gene transfer to airway epithelia In vivo. Am. J. Respir. Cell Mol. Biol. **22:**129–138.
51. **Wang, K., T. Guan, D. A. Cheresh, and G. R. Nemerow.** 2000. Regulation of adenovirus membrane penetration by the cytoplasmic tail of integrin beta 5. J. Virol. **74:**2731–2739.
52. **Wang, K., S. Huang, A. Kapoor-Munshi, and G. Nemerow.** 1998. Adenovirus internalization and infection require dynamin. J. Virol. **72:**3455–3458.
53. **Welsh, R. M., and G. C. Sen.** 1997. Nonspecific host responses to viral infections, p. 109–141. *In* N. Nathason (ed.), Viral pathogenesis. Lippincott-Raven Publishers, Philadelphia, Pa.
54. **Wickham, T. J., P. Mathias, D. A. Cheresh, and G. R. Nemerow.** 1993. Integrins $\alpha_v\beta_3$ and $\alpha_v\beta_5$ promote adenovirus internalization but not virus attachment. Cell **73:**309–319.
55. **Wilmott, R. W., R. S. Amin, C. R. Perez, S. E. Wert, G. Keller, G. P. Boivin, R. Hirsch, J. De Inocencio, P. Lu, S. F. Reising, S. Yei, J. A. Whitsett, and B. C. Trapnell.** 1996. Safety of adenovirus-mediated transfer of the human cystic fibrosis transmembrane conductance regulator cDNA to the lungs of nonhuman primates. Hum. Gene Ther. **7:**301–318.
56. **Worgall, S., P. L. Leopold, G. Wolff, B. Ferris, N. Van Roijen, and R. G. Crystal.** 1997. Role of alveolar macrophages in rapid elimination of adenovirus vectors administered to the epithelial surface of the respiratory tract. Hum. Gene Ther. **8:**1675–1684.
57. **Worgall, S., R. Singh, P. L. Leopold, R. J. Kaner, N. R. Hackett, N. Topf,**

M. A. Moore, and R. G. Crystal. 1999. Selective expansion of alveolar macrophages in vivo by adenovirus-mediated transfer of the murine granulocyte-macrophage colony-stimulating factor cDNA. Blood **93:**655–666.
58. **Yang, Y., Q. Li, H. C. Ertl, and J. M. Wilson.** 1995. Cellular and humoral immune responses to viral antigens create barriers to lung-directed gene therapy with recombinant adenoviruses. J. Virol. **69:**2004–2015.
59. **Yei, S., N. Mittereder, K. Tang, C. O'Sullivan, and B. C. Trapnell.** 1994. Adenovirus-mediated gene transfer for cystic fibrosis: quantitative evaluation of repeated in vivo vector administration to the lung. Gene Ther. **1:**192–200.
60. **Yei, S., N. Mittereder, S. Wert, J. A. Whitsett, R. W. Wilmott, and B. C. Trapnell.** 1994. In vivo evaluation of the safety of adenovirus-mediated transfer of the human cystic fibrosis transmembrane conductance regulator cDNA to the lung. Hum. Gene Ther. **5:**731–744.
61. **Zabner, J., D. M. Petersen, A. P. Puga, S. M. Graham, L. A. Couture, L. D. Keyes, M. J. Lukason, J. A. St. George, R. J. Gregory, A. E. Smith, et al.** 1994. Safety and efficacy of repetitive adenovirus-mediated transfer of CFTR cDNA to airway epithelia of primates and cotton rats. Nat. Genet. **6:**75–83.
62. **Zsengeller, Z. K., S. E. Wert, C. J. Bachurski, K. L. Kirwin, B. C. Trapnell, and J. A. Whitsett.** 1997. Recombinant adenoviral vector disrupts surfactant homeostasis in mouse lung. Hum. Gene Ther. **8:**1331–1344.
63. **Zsengeller, Z. K., S. E. Wert, W. M. Hull, X. Hu, S. Yei, B. C. Trapnell, and J. A. Whitsett.** 1995. Persistence of replication-deficient adenovirus-mediated gene transfer in lungs of immune-deficient (*nu*/*nu*) mice. Hum. Gene Ther. **6:**457–467.